

# Serial Dependence in face-gender classification revealed in low-beta frequency EEG

Giacomo Ranieri<sup>1</sup>, David C. Burr<sup>1,2</sup>, Jason Bell<sup>3</sup> and Maria Concetta Morrone<sup>4</sup>

1. Department of Neuroscience, Psychology, Pharmacology, and Child Health, University of Florence, 50135 Florence, Italy

2. School of Psychology, University of Sydney, Camperdown 2050, Australia

3. School of Psychology, University of Perth, Crawley 6009, Australia

4. Department of Translational Research on New Technologies in Medicine and Surgery, University of Pisa, 56123 Pisa, Italy

CORRESPONDING AUTHOR: David C. Burr. Email: [davidcharles.burr@unifi.it](mailto:davidcharles.burr@unifi.it)

## 15 Abstract

16 Perception depends not only on current sensory input but is also heavily influenced by the  
17 immediate past perceptual experience, a phenomenon known as “serial dependence”. It is  
18 particularly robust in face perception. We measured face-gender classification for a sequence  
19 of intermingled male, female and androgynous images. The classification showed strong serial  
20 dependence (androgynous images biased male when preceded by male and female when  
21 preceded by female). The strength of the bias oscillated over time in the beta range, at 14 Hz  
22 for female prior stimuli, 17 Hz for male. Using classification techniques, we were able to  
23 successfully classify the previous stimulus from current EEG activity. Classification accuracy  
24 correlated well with the strength of serial dependence in individual participants, confirming  
25 that the neural signal from the past trial biased face perception. Bandpass filtering of the  
26 signal within the beta range showed that the best information to classify gender was around  
27 14 Hz when the previous response was “female”, and around 17 Hz when it was “male”,  
28 reinforcing the psychophysical results showing serial dependence to be carried at those  
29 frequencies. Overall, the results suggest that recent experience of face-gender is selectively  
30 represented in beta-frequency (14–20 Hz) spectral components of intrinsic neural oscillations.

31

## 32 Significance Statement

33 The neurophysiological mechanisms of how past perceptual experience affects current  
34 perception are poorly understood. Using classification techniques, we demonstrate that the  
35 gender of face images can be decoded from the neural activity of the EEG response to the  
36 successive face stimulus, showing that relevant neural signals are maintained over trials.  
37 Classification accuracy was higher for participants with strong serial dependence, strongly  
38 implicating these signals as the neural substrate for serial dependence. The best information  
39 to classify gender was around 14 Hz for “female” faces, and around 17 Hz for “male”,  
40 reinforcing the psychophysical results showing serial dependence to be carried at those beta-  
41 frequencies.

42

## 43 Introduction

44 Much evidence has accumulated to suggest that the brain is a prediction machine, which  
45 generates our perceptive experience from internal models based (at least in part) on previous  
46 perceptual experience [1–4]. On this view, the brain must update predictions to minimize the  
47 discrepancy between internal models and external stimuli, in a constantly changing  
48 environment. Recent research suggest that low-frequency neural oscillations are a candidate  
49 for the role of messengers of top-down predictions [5–7].

50 Beta oscillations (13-30 Hz) have been linked to several perceptual, motor and cognitive  
51 processes [8–12]. Especially the lower range (up to ~18 Hz) of beta oscillations may play a  
52 fundamental role in maintenance of working memory [13–15]. Also, they have been  
53 implicated in mechanisms of long-range communication and preservation of current brain  
54 state [16,17]. Top-down beta oscillations to macaque V1 enhance visually driven gamma  
55 oscillations [18]. Betti *et al.* [19] have proposed that beta oscillations may represent long-  
56 term perceptual *priors*. A recent study [20] reports that representations held in working  
57 memory are activated at different phases of a beta (~25 Hz) cycle. In sum, these findings  
58 suggest that beta oscillations may be actively involved in updating priors.

59 Studies suggest that neural representations of recent stimuli linger in visual cortex and are  
60 boosted on the appearance of a coherent stimulus [21–24]. This signal is referred to as an  
61 activity-silent trace, as it seems not to appear in electrophysiological recordings before new  
62 stimulation. It was proposed that the underlying mechanism is a change in synaptic weights  
63 [22,24–27]. Taken together, these findings illustrate a plausible mechanistic model of prior  
64 integration, but the origins, features and dynamics of this perceptual memory trace remain  
65 unclear.

66 To investigate perceptual memory traces and their interaction with neural oscillations, we  
67 applied classification techniques to EEG recordings within a serial dependence paradigm.  
68 Serial dependence is a perceptual phenomenon that reveals the effects of immediate past  
69 experience on the perception of a new stimulus, integrating successive inputs on a perceptual  
70 continuum [28–31]. Liberman *et al.* [32] showed that face identities are subjected to serial  
71 dependence, whereby current perception of a face is systematically pulled towards recently

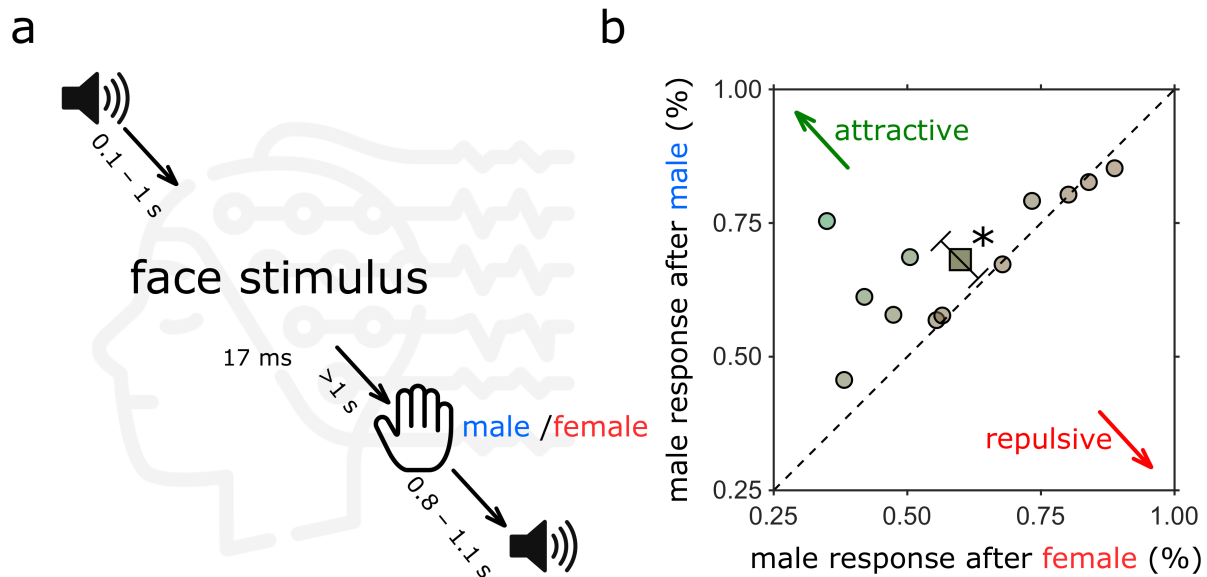
72 seen faces [33]. Bell *et al.* [34] showed that oscillatory activity in the beta range plays an  
73 important role in discrimination of gender, and that the oscillation frequency differs between  
74 male and female images: faster for male biases (17 Hz) and slower for female biases (~13 Hz).  
75 Based on these findings, we used a face-gender discrimination paradigm to study the  
76 neurophysiological characteristics of information of perceptual history embedded in neural  
77 oscillations. We classified previous responses across narrow-band frequency ranges, showing  
78 that the correlation of EEG signal and serial dependence peaks at separate frequencies for  
79 trials with high male and high female bias. Peak frequencies of the correlation were higher  
80 for male and lower for female images, consistent with frequencies identified in behavioral  
81 analysis.

82

## 83 Results

### 84 ***Behavioral results (serial dependence and oscillations in bias)***

85 Twelve participants (5 female) were asked to classify a sequence of face images as *Male* or  
86 *Female* (Fig. 1A and methods). The images were of three types, male, female and  
87 androgynous, constructed from morphed face space. Despite calibration, aiming at 25, 50 and  
88 75% response for female, male and androgenous stimuli, there remained a tendency to  
89 respond male rather than female to androgynous faces (average proportion male response =  
90  $0.62 \pm 0.14$  STD). Considering only androgynous trials, participants responded *Male* more  
91 often when the previous response was *Male* rather than *Female*, consistent with a significant  
92 serial dependence effect (Fig. 1b: average difference =  $0.082 \pm 0.13$  STD, paired-ttest  
93  $p = 0.044$ ). The effect varied considerably across subjects, suggesting genuine individual  
94 differences, consistent with previous studies [35,36]. Separating participants based on their  
95 gender did not reveal any meaningful difference in overall bias (average proportion male  
96 response for female participants =  $0.68 \pm 0.21$  STD, average proportion male response for  
97 male participants =  $0.58 \pm 0.11$  STD).



98

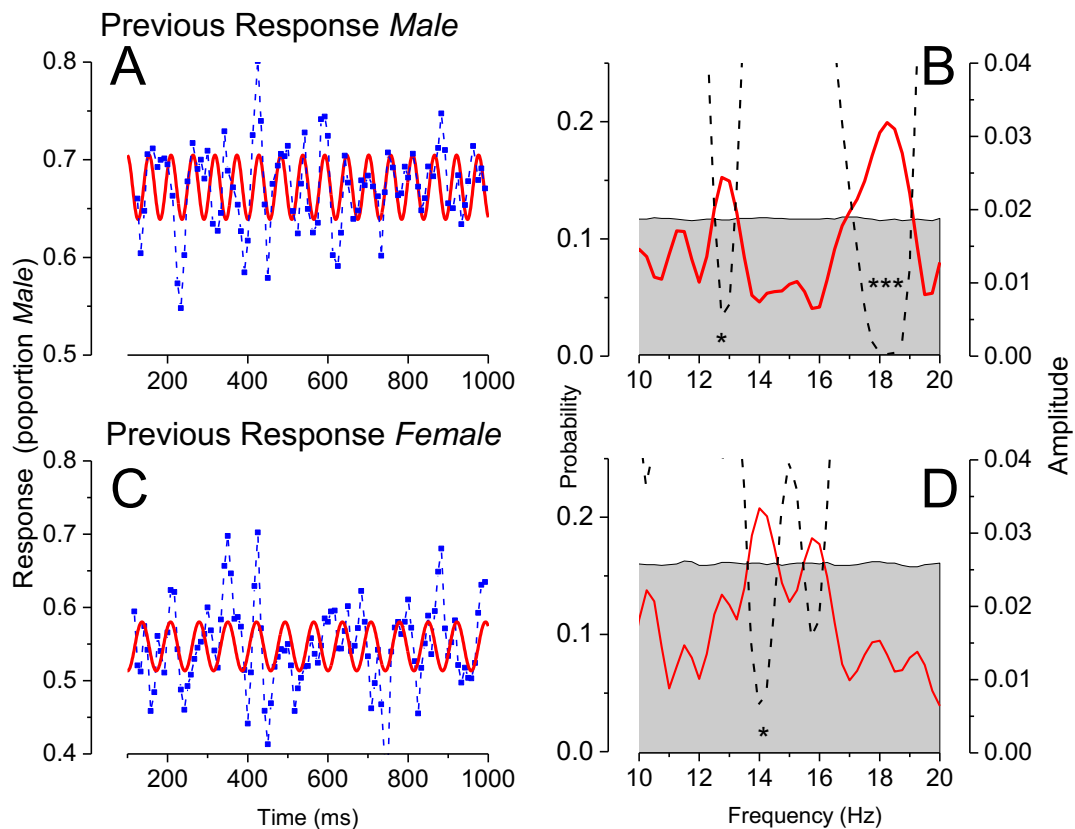
99

Figure 1

100 Experimental paradigm and behavioural results. **A.** Schematics of the experimental paradigm. Each trial started  
101 with an audio cue followed after a random interval (between 100 -1000 ms) by a face image for 2 screen frames  
102 (16.6 ms). There were 15 different face identities, each morphed into 3 genders (androgynous, female and male),  
103 making 45 faces in total. Participants waited at least 1 s before responding by key-press, indicating whether the  
104 face appeared more female or male. A new trial started after an inter-trial interval between 800 and 1100 ms.  
105 **B.** Proportion male responses to androgynous stimuli, depending on the response to the previous stimulus  
106 (response “female” plotted on abscissa, “male” on ordinate). Yellow circles represent individual participants, with  
107 the dark yellow diamond showing the average participant. Participants above and to the left of the equality line  
108 tend to respond more male if the previous was male, and vice versa (positive serial dependence). The average  
109 participant showed serial dependence (average difference in proportion male response =  $0.08 \pm 0.13$ ,  $p = 0.04$ ).

110 As shown in Figure 1A, each trial was initiated with an auditory tone, followed by the face  
111 stimulus after an interval ranging from 100 to 1000 ms. This procedure aimed to reveal  
112 oscillations in the response, as salient auditory stimuli can reset the phase of endogenous  
113 oscillations [37]. Figures 2A & C show the oscillatory biases in responses, plotted as a function  
114 of time after the synchronizing auditory tone, separately for when the previous response was  
115 *Male* and *Female*. In both cases the responses were not constant, but oscillated over time,  
116 faster for preceding *Male* than *Female* stimuli. The red curves of Figures 2A&C show the best-  
117 fitting sinusoids, and Figures 2B&D show the associated Fourier transforms. Following a male  
118 response, bias oscillated at 18.2 Hz ( $p < 0.005$ , corrected for all frequencies in the range 10-  
119 20 Hz of the surrogate data: see Methods), and also, but less significantly at 13 Hz ( $p < 0.05$ ).  
120 Following a female response, bias oscillated most strongly at 14 Hz (significance  $p < 0.05$ ).  
121 These results replicate the findings of Bell et al. (2020), where bias synchronized to voluntary  
122 button press (possibly a stronger endogenous reset) oscillated at 17 Hz after for previous male  
123 faces, and 13.5 Hz for female faces.

124



125

126

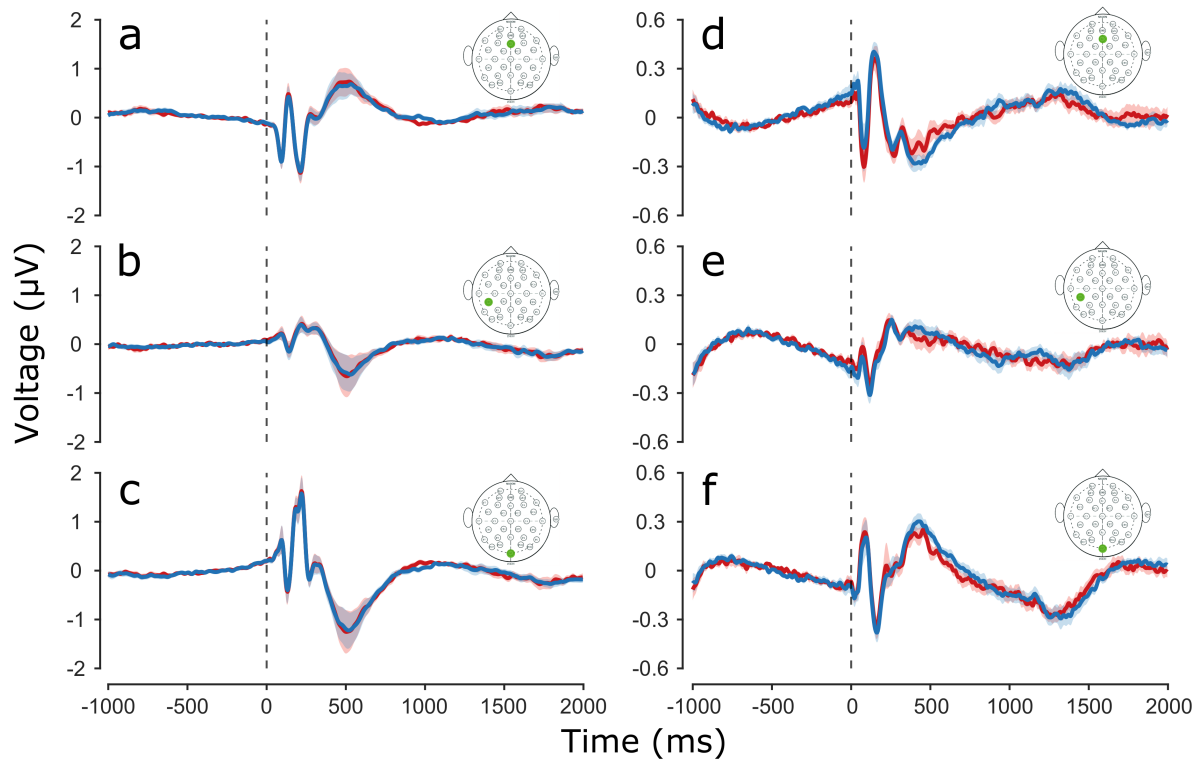
**Figure 2**

127 Timecourse and Fourier transforms of response bias. **A.** Proportion of “Male” responses to androgynous stimuli  
128 preceded by response *Male*, as a function of time after the auditory tone (blue symbols). The red curve shows the  
129 best fitting sinusoid, at 18.2 Hz. **B.** Fourier transform of the data of Fig. A, showing the strongest peak at 18.2 Hz.  
130 There is a secondary, weaker peak at 13 Hz. The dashed black lines show probability of significance, corrected  
131 for all frequencies in the range 10-20 Hz of the surrogate data **C.** Same as A, but for stimuli preceded by response  
132 *Female*. Best fitting sinusoid at 14 Hz. **D.** Same as B, for stimuli preceded by response *Female*.

133

### 134 **EEG results (ERP and power analysis)**

135 The main purpose of this study was to study the neural mechanisms behind serial  
136 dependence, recording EEG from participants while they made sequential psychophysical  
137 judgements. We first analyzed the ERPs for the two conditions “previous response male” and  
138 “previous response female” (average result in Fig. 3 a-c for electrodes Fz, CP5 and Oz). There  
139 were no clear or significant differences between the two conditions. We also analyzed the  
140 responses aligning them to the phase-resetting auditory tone (Fig. 2 d-f), but again, there  
141 were no significant differences in the responses.



142

143

**Figure 3**

144 Event-related potentials (ERPs) separated according to previous response. **A-C.** ERP synchronized to face  
145 stimulus presentation of example Fz, CP5 and Oz electrodes. In blue ERP of trials where participants responded  
146 male to the previous trial, in red where they responded female. Color shading represents  $\pm$ Standard Error of the  
147 Mean (SEM). **D-F.** ERP synchronized to audio cue presentation of Fz, CP5 and Oz electrodes.

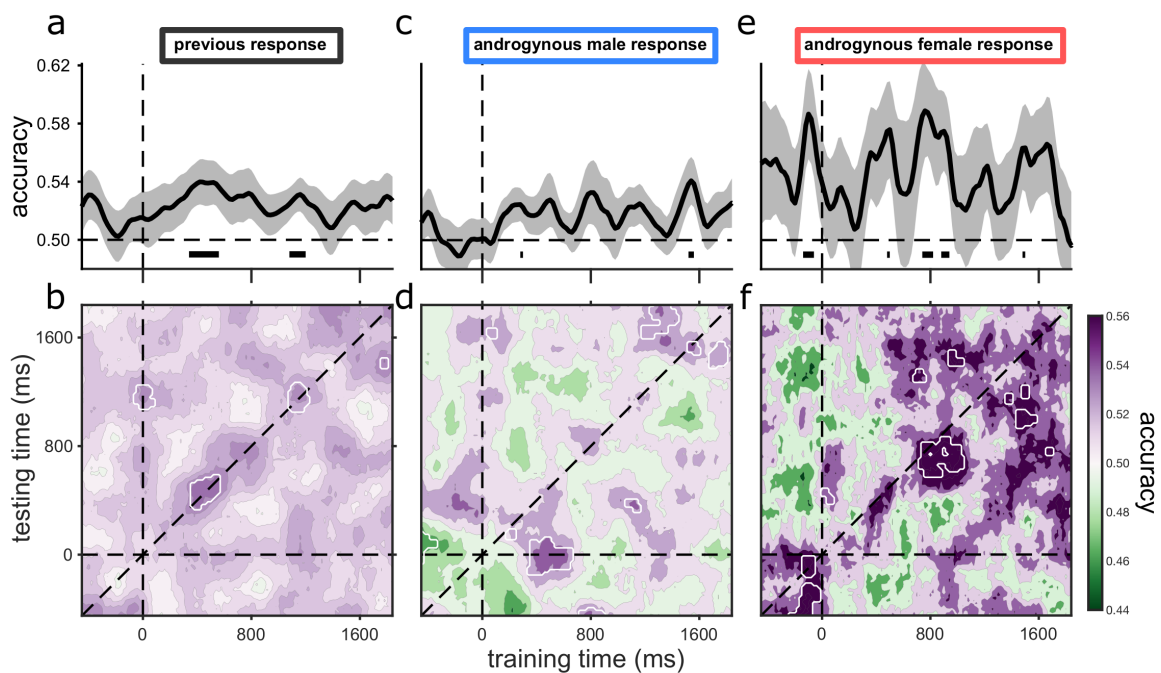
148

### 149 **Decoding results**

150 We next used classification techniques to test whether decoding EEG signals to the current  
151 trial could classify the responses to the *previous* face stimuli. This technique is based on small  
152 differences in signal distribution across electrode position. It relies on few assumptions, as all  
153 brain activity is used, without selecting electrodes or ROIs.

154 Figure 4a shows the main result. It shows accuracy of decoding the *previous* psychophysical  
155 response from the EEG response to the current stimulus, as a function of time after (current)  
156 stimulus onset. The curve is consistently above chance (0.5, for the two possible responses),  
157 and reaches the stringent significance level between 340 and 560 ms after stimulus onset,  
158 and also between 1080 and 1200 ms. This shows that there is information about the *previous*  
159 trial in the neural response to the current trial. Figure 4b is the temporal generalization matrix

160 showing classification accuracy across all training and testing times. The decoding  
161 performance of the trained models for the specific time interval is plotted as a heat map.  
162 There are three regions where decoding was significantly above chance (within the white  
163 regions of Fig. 3b), two corresponding to those illustrated in Figure 4a (which is the diagonal  
164 of the matrix), and an extra one at 0 training and about 120 ms testing. The regions of high  
165 accuracy are distributed mainly across the diagonal, but the additional significant region away  
166 from the diagonal is evidence for some generalization for different training and testing times.



167

168

**Figure 4**

169 Decoding of previous responses from current-trial EEG activity. In all decoding procedures, classifiers were  
170 trained to distinguish between previous response male and previous response female, on all trials. **A.** Classifier  
171 accuracy as a function of duration after trial onset for all trials of the previous stimuli. **B.** Generalization matrix  
172 for the same stimuli, decoding all possible combinations of training and testing times. White contours indicate  
173 regions of significant accuracy after cluster correction. Decoding was strongest along the diagonal (which  
174 corresponds to figure A), but there were also significant regions of decoding away from the diagonal, suggesting  
175 generalization of decoding. **C,D** Same as A & B, but only when the current response was male and the previous  
176 stimulus androgenous. **E,F** Same as A & B, but only when the current response was female and the previous  
177 stimulus androgenous.

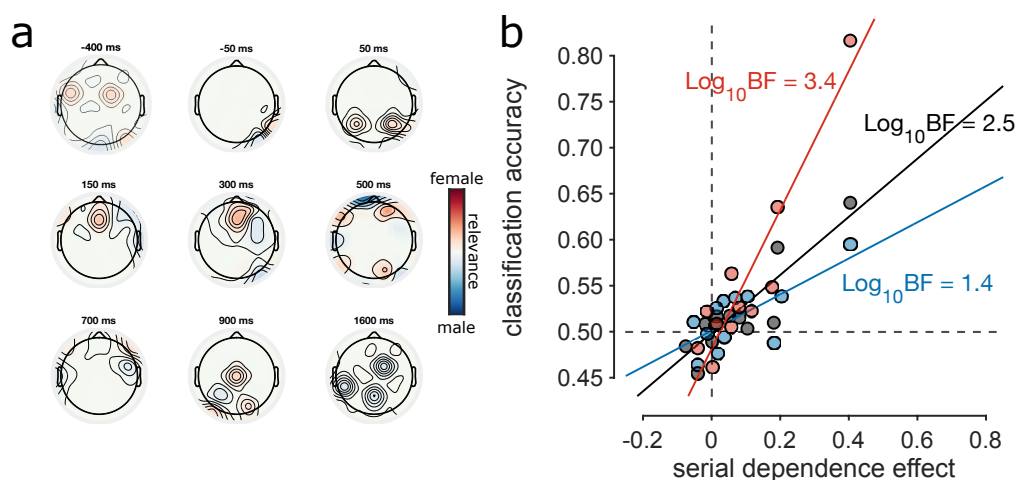
178

179 To investigate further the relevance of this trace on participant responses, we considered only  
180 trials where the current stimulus was androgynous, and further separated them on the basis  
181 of participant response to it (male or female: Fig. 4c–f). We took classifiers trained on all

182 *previous* trials (as for Fig. 4a&b), but tested them on these two subsets of data: current  
183 androgenous stimuli with response *Male* and with response *Female*, to examine separately  
184 decoded signal in trials where participants had higher likelihood of being biased towards one  
185 of the two responses based on the presence of the memory trace.

186 The results show that previous response traces are much more readable in androgynous trials  
187 where participants responded *Female* (difference in peak accuracy =  $0.12 \pm 0.03$  SEM,  
188  $p = 0.003$ ,  $\text{Log}_{10}(\text{BF}_{10}) = 1.16$ ). This is possibly due to the overall tendency of participants to  
189 respond male, so there is more information in a response *Female*. Again the highest accuracy  
190 tends to be on the diagonals, but some regions off-diagonal are significant, pointing to limited  
191 generalization of coding and decoding.

192 Activation maps (Fig. 5a) show the time-course of which electrodes were most informative  
193 for classification. Before stimulus presentation decoding relied on a stable right-occipital  
194 dipole and on distributed frontocentral locations. In early perceptual processing (up to  
195  $\sim 60$  ms) the memory signal was classified by activity of occipital electrodes. The signal shifted  
196 progressively to frontal locations up to 140 ms, when just frontal electrodes contributed to  
197 classification. At 300 ms, occipital electrodes started to contribute again to the signal. At  
198 around 700 ms parietal and frontocentral locations became relevant, remaining relatively  
199 stable up to about 1600 ms. Activation maps before stimulus presentation and well after  
200 stimulus presentation were quite different, consistent with the lack of generalization for  
201 those intervals across training and testing time (Fig. 4 b,d,f top-left and bottom-right corner).



202

203

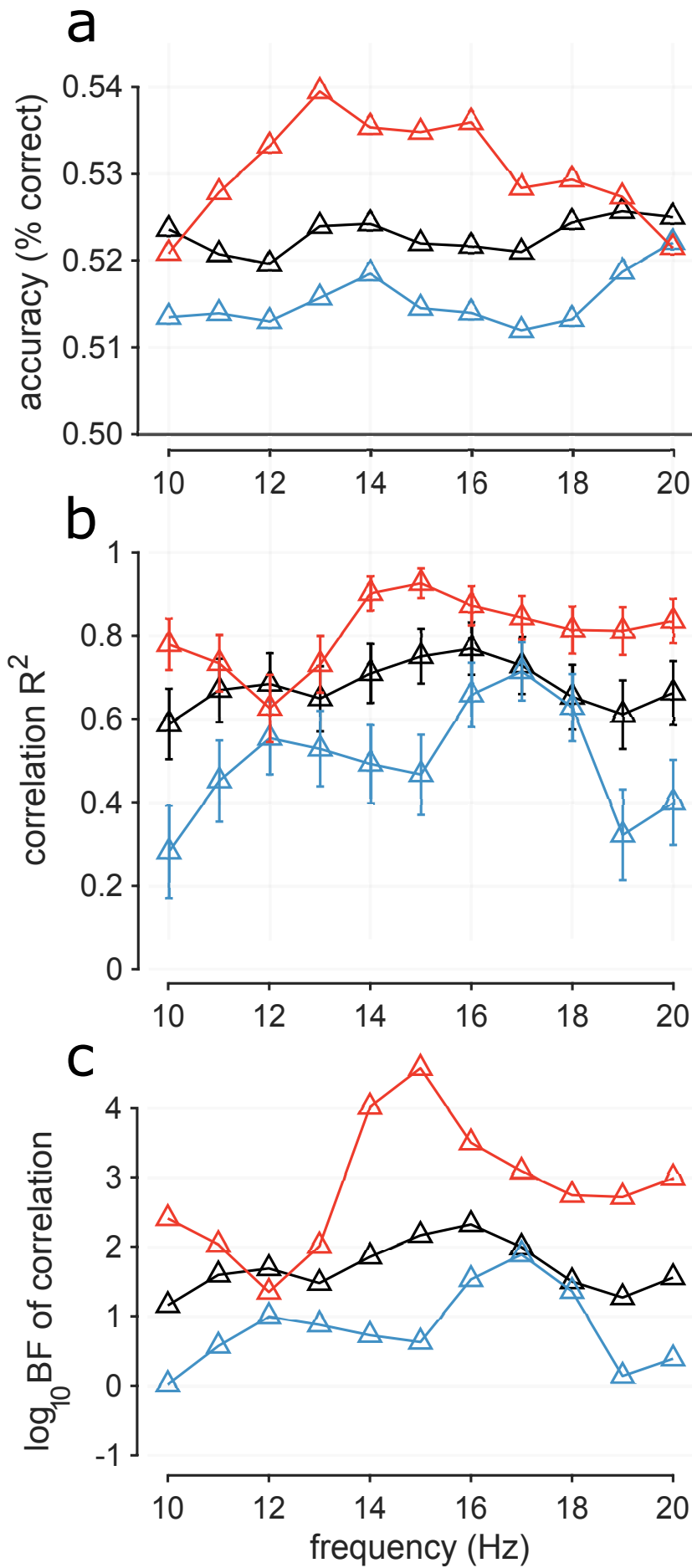
Figure 5

204 Activation patterns and correlation with behavior. **A.** Activation patterns of classification showing the relative  
205 weights assigned to electrodes for decoding for example time points. Positive weights (red) indicate that higher  
206 power at the location sways classifiers to identify the signal as belonging to the “previous female” class, while  
207 negative weights (blue) indicate that higher power sways classification towards “previous male”. Weights are  
208 normalized on maximum activation across electrodes and time. **B.** Correlation between serial dependence strength  
209 and classification accuracy across participants, for the 3 decoding conditions in Fig. 3. Serial dependence strength  
210 (abscissa, constant across all 3 conditions) was calculated as the difference between proportion male response  
211 with previous male response and proportion male response with previous female response. Classification accuracy  
212 was calculated by averaging individual participant accuracy across the diagonal  $\pm 2$  points (final precision  $\pm 60$   
213 ms) in the window 0–1 s. Decoding tested on all trials in black, on androgynous trials with female response in red,  
214 on androgynous trials with male response in blue. The strength of the correlation is given by  $\text{Log}_{10}$  Bayes Factor,  
215 shown near each fit.

216

217 We tested the correlation between classification accuracy and serial dependence across  
218 participants (Fig. 5b). Classification accuracy was averaged over the entire post-stimulus time  
219 window of the temporal generalization matrix, and serial dependence calculated as the  
220 difference of proportion male responses on androgynous trials when the previous response  
221 was male compared with when it was female. We found a significant positive correlation of  
222 serial dependence with average decoding of all trials (black dots,  $r = 0.89$ ,  $p < 0.001$ ,  
223  $\text{Log}_{10}\text{BF} = 2.5$ ). The correlation of memory trace and serial dependence was stronger for  
224 classification accuracy of female-biased trials (red dots,  $r = 0.93$ ,  $p < 0.0001$ ,  $\text{Log}_{10}\text{BF} = 3.4$ )  
225 compared with male-biased trials (blue dots,  $r = 0.80$ ,  $p = 0.002$ ,  $\text{Log}_{10}\text{BF} = 1.4$ , but the  
226 difference was not statistically different ( $r_{\text{difference}} = 0.13$ ,  $p = 0.23$ ).

227 To relate the EEG results to the psychophysics, which showed clear beta-frequency  
228 oscillations, we repeated the decoding analysis after filtering the EEG into narrow-band  
229 windows, from 4 to 20 Hz. Figure 6A shows how decoding accuracy varied with filter  
230 frequency. Considering all androgenous stimuli, average classification was relatively flat  
231 across frequency (black dashed line, Fig. 6a). However, confining the analysis to androgynous  
232 stimuli with female response shows slightly decoding around low-beta, 12-17 Hz (red line,  
233 Fig. 6). The trend with androgynous stimuli with male response was less clear, but tended to  
234 increase over the beta range, peaking at the maximum analyzed, around 20 Hz. This is  
235 consistent with the psychophysical results, but not strong support.



237

### Figure 6

238 Decoding across narrow frequency ranges. **A.** Classification accuracy across frequency calculated as average  
239 across the diagonal  $\pm 2$  points (precision  $\pm 60$  ms) in the window 0–1 s. Classification accuracy tested on all trials  
240 (black), on androgynous trials with female response (red) and on androgynous trials with male response (blue).  
241 **B.** Squared correlation coefficients (variance explained) between classification accuracy and serial dependence  
242 strength across participants. Classification accuracy calculated as in A. Serial dependence effect (constant across  
243 all 3 conditions) was calculated as the difference between proportion male response with previous male response  
244 and proportion male response with previous female response. **C.** Log<sub>10</sub> of bayes factor of the correlations of  
245 Fig. B.

246

247 As decoding accuracy covaried with the magnitude of serial dependence, showing a strong  
248 link between the psychophysics and EEG, we next tested whether the strength of the  
249 correlation may vary with frequency range. Figure 6b shows how the square of the correlation  
250 coefficient ( $R^2$ , the variance explained by the correlation) varies with filter frequency. The  
251 correlation considering all androgenous trials are again relatively flat, but the correlation for  
252 the androgenous stimuli with *Female* response shows peaks at around 14-15 Hz, while that  
253 for androgenous stimuli with male response peaks at 17 Hz. Again this is very similar to the  
254 psychophysical results showing peaks at 14 and 18 Hz for previous *Female* and *Male*  
255 responses. Figure 6C shows the log Bayes Factor associated with the correlations, showing  
256 even clearer peaks at 14 Hz for *Female* and 18 Hz for *Male*.

257

## 258 Discussion

259 This study investigated whether neural endogenous oscillations may be instrumental in  
260 transmitting predictive information about face-gender. The results show that previous  
261 responses leave a lingering EEG trace that can be decoded during the processing of a new  
262 stimulus. We report strong correlations between the strength of behavioral serial  
263 dependence effects and the strength of neural classification of previous responses.  
264 Importantly, the correlations peak at similar frequencies to those identified in behavioral  
265 analysis, both in previous research [34] and here, suggesting that perceptual representations  
266 of recent experience may be encoded within the spectral structure of neural oscillations.

267 Since classifiers are trained on averages of single-trial EEG amplitude envelopes, decoding  
268 could rely on both phase-locked and non-phase-locked information. Temporal generalization

269 maps reveal sparse regions of significant decoding of the previous response, but exploring the  
270 distributions of accuracy, especially for androgynous trials with female response, suggests  
271 that regions of high accuracy may be distributed over the entire temporal matrix, rather than  
272 being confined to the diagonals where training and testing time coincide. This qualitative  
273 interpretation would be consistent with a memory signal that is relatively stable in time, with  
274 discrete evolution at specific time points [38]. Decoding accuracy was strongest for  
275 androgynous trials with female response, and weakest for androgynous trials with male  
276 response. This may be explained by the overall male bias of participants, so the female  
277 response was more informative.

278 To demonstrate decoding of previous trials, we chose to use responses rather than stimuli as  
279 class labels, for several reasons. Firstly, on half the trials the stimuli were androgynous,  
280 neither male nor female, and therefore uninformative: yet the response to those stimuli is  
281 very informative, reflecting an internal state rather than the stimulus. Secondly, as responses  
282 to male and female stimuli were about 75% correct, stimuli and responses are highly  
283 correlated, hard to disentangle. We are aware of the ongoing debate on whether serial  
284 dependence acts on early perception or on later decision-making processes [39–43].  
285 However, responses do not represent only late decision stages, but the internal neural state  
286 of the participant, so the choice of using responses does not speak to this issue. Inspection of  
287 the activation patterns of decoders shows that classification relies mainly on occipital  
288 electrodes during early stages of visual processing. This is consistent with quick activation of  
289 early visual cortices reported in previous studies on serial dependence [41,44–46]. The  
290 immediate activation of visual areas, as early as 50 ms after face presentation (earlier than  
291 we would expect for bottom-up visual processing) suggests that the representation of the  
292 prior may be already embedded in visual cortices, possibly in the form of synaptic gain  
293 changes [22,23,47]. Lastly, the correlation between neural signal and behavior and the  
294 coherence in frequency found in the GLM analysis points to beta oscillations as the generator  
295 of the behavioral bias.

296 Recent studies have employed classification techniques to reveal traces of previous trials,  
297 suggesting that perceptual experience lingers as an activity-silent trace, which is then  
298 reactivated with new stimulation [21–24]. In these paradigms, classification accuracy is at  
299 chance level before the presentation of a new stimulus, and significant decoding is reported

300 only after. However, researchers have also questioned the activity-silent trace hypothesis.  
301 Runyan *et al.* [48] identified replay of neural activity during rest, which may be related to  
302 ongoing consolidation processes that help to strengthen memories over time. Stokes *et al.*  
303 [49] also challenge the idea, suggesting that perceptual learning is instead supported by  
304 changes in neural connectivity and plasticity. We have previously supported the activity-silent  
305 trace hypothesis [24], finding that classification accuracy (for spatial frequency  
306 discrimination) was not significant before new stimuli were presented. However, the  
307 temporal generalization matrices (Fig. 3) for the female bias condition show that the trace is  
308 sometimes present before the presentation of a new stimulus. However, in interpreting these  
309 results, we also have to consider that the generalization matrices for female bias is noisier,  
310 given the lower number of trials available. Furthermore, classifiers trained before time 0 do  
311 not accurately classify previous traces after time 0, and vice versa. This suggests that there is  
312 a distinct change in the signal when a new stimulus is presented, supporting the action of a  
313 silent memory signal.

314 It is widely acknowledged that observers enhance efficiency by using past information to  
315 anticipate future sensory input. The connection between behavior and decoding of previous  
316 responses was notably pronounced when limiting the neurophysiological signal to low-beta  
317 frequencies, where the behavioral bias oscillated according to the previously perceived  
318 gender. It has been established that low-frequency oscillations contribute to the transmission  
319 of predictive information, akin to the concept of perceptual echoes put forth by VanRullen &  
320 Macdonald [50]. Ho *et al.* [51] showed that auditory stimuli oscillated within the alpha range  
321 (~9 Hz) at distinct phases when presented to either the left or the right ear. Using a similar  
322 paradigm to the present study, Bell *et al.* [34] demonstrated that following the observation  
323 of a specific stimulus, whether male or female, the inclination to perceive an androgynous  
324 face as female or male oscillated respectively at 13.5 or 17 Hz. Considerable evidence exists  
325 detailing how bias exhibits oscillatory behavior at specific frequencies, as observed in visual  
326 orientation discrimination [36], trans-saccadic location discrimination [52], audiovisual  
327 temporal judgement [53]. For more intricate perceptual functions, like face gender  
328 discrimination, it is possible that prior expectations require a coding mechanism involving  
329 multiple frequency channels. The literature suggests that beta oscillations may play a role in  
330 processing local features [54,55]. It is conceivable that various frequencies of beta oscillations

331 might explain the response patterns elicited by female or male stimuli, as well as more  
332 complex stimuli in general. The arrangement of local facial features could potentially clue the  
333 interpretation of faces as masculine or feminine.

334 Overall, our results suggest that recent experience of face-gender is represented in low-  
335 frequency spectral components of intrinsic neural oscillations (low-beta 14–20 Hz). The  
336 strength of the active trace correlates with the strength of serial effects in behavior, especially  
337 in the low-beta range, suggesting that our signal may be the underlying neural substrate of  
338 the attractive effect. These results suggest that recent experience lingers in perceptual  
339 cortices and changes with new stimulation, possibly becoming strengthened. The strong  
340 correlation between decoding accuracy and the strength of serial dependence further  
341 suggests that these oscillatory signals are highly instrumental in the transmission of internal  
342 models, within the predictive coding framework [5,56]. Overall, our results corroborate the  
343 intuition of Bastos *et al.* [57] that in a hierarchical predictive coding framework, low-  
344 frequency neural oscillations in encephalography (4–22 Hz range) are a good candidate for  
345 top-down internal models.

346

## 347 **Materials and Methods**

### 348 ***Participants***

349 Twelve healthy adults (7 females, age range 20 – 29 years, mean = 24.8 years, SD = 2.7 years)  
350 participated in the experiment with monetary compensation (10 €/h). All participants had  
351 normal or corrected-to-normal vision and gave written informed consent. The experimental  
352 design was approved by the local regional ethics committee (*Comitato Etico Pediatrico  
353 Regionale — Azienda Ospedaliero-Universitaria Meyer — Firenze*), and is in line with the  
354 declaration of Helsinki for ethical principles for medical research involving human subjects  
355 (DoH-Oct2008). We did not perform a formal power analysis to determine participant number  
356 but, based on our previous experience with decoding EEG [24] and also psychophysically  
357 measured oscillations of face gender [34], we reasoned that 12 should be sufficient.

### 358 ***Stimuli and apparatus***

359 The experiment was recorded in a quiet dark room, where participants sat in a comfortable  
360 chair with head rested on a chin rest. The stimuli were presented on a Display++ LCD Monitor  
361 (Cambridge Research Systems, 120 Hz, 1920 x 1080 resolution), gamma corrected, 70 cm from  
362 the eyes, mean grey screen luminance equal to 50 cd/m<sup>2</sup>. Face stimuli were a subset of images  
363 taken from Bell et al. (2020). They were originally generated in FaceGen Modeller 3.5.3 and  
364 saved as high resolution 2D grey scale image (6.6° x 6.6°). The faces were white, mid 20s, with  
365 gender neutral coloring, shape, and typical asymmetry. We performed a preliminary  
366 response-balancing procedure on 4 naïve observers who did not participate in the experiment  
367 (600 trials each, 25 face identities). We selected 15 face identities based on mean response  
368 deviating no more than ±10% from target accuracies (75% male response for male faces, 50%  
369 male response for androgynous, 25% male response for female). The phase-resetting auditory  
370 stimulus was a 16 ms, 900 Hz pure tone (80 dB sound pressure level at the ear, 44100 kHz  
371 sampling frequency) projected through 2 loudspeakers besides the monitor (following Romei  
372 *et al.* [37]).

### 373 ***Procedure***

374 Participants fixated a white fixation dot at the center of the screen, which was present for the  
375 whole duration of the experiment except during face stimulus presentation. Each trial began  
376 with the presentation of the auditory stimulus. After an interval ranging uniformly from 100  
377 to 1000 ms (at 120 Hz sampling frequency, the monitor refresh rate) one of the 45 faces was  
378 presented for 17 ms (two frames). Participants were instructed to wait at least 1 second  
379 before responding, indicating whether the presented face seemed male or female (by  
380 pressing the left or right arrow keyboard keys). Trials where participants responded earlier  
381 than 1 second were eliminated from the analysis. Response configuration (association of  
382 arrows with gender) was randomized between participants, and switched halfway through  
383 the experiment. After button press, a new trial started after an interval ranging uniformly  
384 from 800 to 1100 ms, so that the auditory stimulus presentation was not easily predictable.  
385 Each participant completed 1215 trials.

### 386 ***EEG Acquisition and Preprocessing***

387 EEG data were collected with a Nautilus Research headset (g.tec) at a sample rate of 250 Hz  
388 with no online filtering. The data were referenced online to a unilateral electrode placed  
389 behind the left ear. Activity was measured from 32 gel-based active electrodes (g.LADYbird  
390 technology) arranged according to the 10/20 system. Impedance was kept below 50 k $\Omega$ .

391 Offline EEG preprocessing was performed in MATLAB (MathWorks®) with custom code. EEG  
392 data were referenced to the common average reference and filtered with a FIR bandpass filter  
393 (Chebyshev window, 128<sup>th</sup> order, stopbands 1 Hz and 35 Hz, sidelobe magnitude factor 50  
394 dB). For the main data analysis, epochs were extracted aligned to stimulus presentation,  
395 comprising a segment of data from –500 ms to 1800 ms after the stimulus. Epochs were  
396 visually inspected for motor artifacts and wireless failure of signal transmission (manual  
397 rejection of 0.8%  $\pm$  0.6% STD of data across subjects). Ocular artifacts were removed through  
398 blind source separation with ICA decomposition [58].

### 399 ***Data analysis – psychophysics***

400 We analyzed individual responses to androgynous face identities, calculating the proportion  
401 of “male” responses, depending on the response to the previous trial. We removed from all  
402 analyses trials where response latencies were lower than 1 second or higher than 3 seconds  
403 (average response latency 2.2 s; CI95 = 1.6–2.7 s). After artifact removal we obtained 1249  $\pm$  9  
404 trials per subject. To assess whether previous responses changed gender discrimination bias,  
405 we compared by t-test proportion “male” responses when previous response was male to  
406 when previous response was female (only on androgynous trials). The same analysis was  
407 repeated based on face identity of the previous trial (stimulus-based analysis).

408 To measure oscillations in face-gender behavioral bias, we applied single-trial analysis to  
409 aggregate data from all participants, including all the trials that survived the EEG artefact  
410 rejection procedure. The general linear model (GLM) analysis weighted each single trial with  
411 the following model:

$$412 \quad y = \beta_0 + \beta_1 \sin(2\pi ft) + \beta_2 \cos(2\pi ft) \quad \text{eq. 1}$$

413 where  $y$  is participant response (1 for male, 0 for female),  $t$  is SOA (audio to face) in seconds,  
414  $f$  is a fixed frequency ranging from 4 to 20 Hz at 0.5 Hz intervals,  $\beta_0$ ,  $\beta_1$  and  $\beta_2$  are free

415 parameters. We separated responses to all stimuli based on previous response (male or  
416 female), and fit the above GLM, calculating the amplitude of the sinusoidal fit to each  
417 frequency in the range 10-20 Hz. To assess statistical significance, the surrogate data  
418 generated by shuffling the responses (2000 permutations) were analyzed with the same GLM  
419 obtaining a distribution of amplitudes across frequencies under the null hypothesis.  
420 Frequencies with amplitudes over the 95<sup>th</sup> percentile of this distribution were candidates for  
421 statistical significance. Candidate frequencies were deemed statistically significant only if they  
422 were included in a cluster larger than the 95<sup>th</sup> percentile of the distribution of cluster sizes.  
423 For each cluster in both previous male and previous female conditions, we noted the local  
424 maxima of amplitudes and their corresponding frequencies. For illustration purpose only  
425 (Fig. 6) we show the responses binned on stimulus onset asynchrony (SOA) at 8.3 ms intervals  
426 with a running average of 3 consecutive bins (weights: 0.305, 0.39, 0.305).

#### 427 ***Data analysis – EEG time-domain and power analysis***

428 We calculated event-related potentials (ERPs) synchronized to face stimulus presentation,  
429 separately for the two conditions “previous male” and “previous female”. Grand-average  
430 ERPs were calculated by averaging single-participant ERPs normalized (z-scores) to a baseline  
431 window in the interval from –500 to –100 ms with respect to stimulus presentation.

432 We classified previous ( $n-1$ ) responses from the EEG activity elicited by the current ( $n$ ) trial.  
433 Before classification, we filtered the entire time series of  $111 \pm 18$  minutes across participants,  
434 in a low-beta range (14 to 20 Hz) and calculated the amplitude of the analytic envelope using  
435 the Hilbert transform (Fig. 3). For the second decoding procedure (Fig. 5) we filtered narrowly  
436 around frequencies from 4 to 20 Hz at 1 Hz steps (Type II Chebyshev window, 1024<sup>th</sup> order,  
437 passband 0.5 Hz above and below the selected frequency, stopband 1 Hz above and below  
438 the selected frequency, sidelobe magnitude factor 50 dB). We down-sampled trials to 50 Hz,  
439 obtaining 150 time points from –500 to 1000 ms, synchronized to face stimulus presentation.  
440 To boost signal-to-noise ratio, we averaged 5 trials of the same class together (as in Foster et  
441 al., 2016), obtaining our final classification samples. We used binary support vector machine  
442 (SVM) classifiers with linear kernel (the MATLAB *fitcsvm* function), using the 32 electrode  
443 locations as features for classification. Samples were split in 5 folds, with a 4:1 training to  
444 testing ratio ( $196 \pm 14$  SD samples in the training set per observer). The procedure was

445 repeated 5 times, rotating which fold was used for testing. The whole decoding procedure  
446 was repeated 100 times, generating new samples every time by averaging random sets of 5  
447 trials together. This allowed us to minimize lucky splits of the data and assess accuracy by  
448 averaging over a large number of guesses ( $24,519 \pm 141$  SD guesses per observer).

449 We assessed temporal generalization by testing classifiers across all time points, obtaining a  
450 matrix of accuracy across training and testing times per participant. We averaged accuracy  
451 across participants and extracted matrix diagonals to show the dynamics of previous response  
452 signals. Statistical power was defined by t-tests against 50% accuracy across training and  
453 testing time. To correct for multiple comparisons, we permuted class labels at the level of  
454 testing, obtaining a set of 2000 temporal generalization matrices under the null hypothesis.  
455 For each matrix, we noted how many adjacent points survived a t-test against 50% accuracy,  
456 generating a distribution of cluster sizes. Calculating the 95<sup>th</sup> percentile of this distribution,  
457 we obtained a threshold of cluster size. All clusters smaller than the identified thresholds were  
458 deemed non-significant.

459 Activation patterns show the relative relevance of electrode sites for classification, giving  
460 qualitative insight on model dynamics. Activation patterns were calculated as follows:

$$461 \quad A = \beta * X^T \quad \text{eq. 2}$$

462 Where  $\beta$  are classifier coefficients and  $X^T$  is the transposed matrix of EEG signal of tested data.

463 Classifiers trained on all trials were then tested on 2 subsets of trials: androgynous trials to  
464 which observers responded “male” and androgynous trials which observers responded  
465 “female”. Class labels within these conditions were again responses to the previous trial. As  
466 trials in the two conditions are likely trials where serial biases were more present, this testing  
467 procedure highlighted whether the information is stronger in male-biased or female-biased  
468 trials.

469

470

## 471 References

472 1. Gregory RL. 1980 Perceptions as Hypotheses. *Philos. Trans. R. Soc. Lond. B. Biol.*

- 473            *Sci.* **290**, 181–197.
- 474    2.    Clark A. 2013 Whatever next? Predictive brains, situated agents, and the future of  
475            cognitive science. *Behav. Brain Sci.* **36**, 181–204. (doi:10.1017/S0140525X12000477)
- 476    3.    Friston K. 2010 The free-energy principle: a unified brain theory? *Nat. Rev. Neurosci.*  
477            **11**, 127–138. (doi:10.1038/nrn2787)
- 478    4.    Cicchini GM, Mikellidou K, Burr DC. 2018 The functional role of serial dependence.  
479            *Proc. R. Soc. B Biol. Sci.* **285**. (doi:10.1098/rspb.2018.1722)
- 480    5.    Friston KJ. 2019 Waves of prediction. *PLoS Biol.* **17**, e3000426.  
481            (doi:10.1371/journal.pbio.3000426)
- 482    6.    Benedetto A, Binda P, Costagli M, Tosetti M, Morrone MC. 2021 Predictive visuo-  
483            motor communication through neural oscillations. *Curr. Biol.* **31**, 3401–3408.e4.  
484            (doi:10.1016/j.cub.2021.05.026)
- 485    7.    Turner W, Blom T, Hogendoorn H. 2023 Visual Information Is Predictively Encoded  
486            in Occipital Alpha/Low-Beta Oscillations. *J. Neurosci.* **43**, 5537 LP – 5545.  
487            (doi:10.1523/JNEUROSCI.0135-23.2023)
- 488    8.    Kühn AA, Williams D, Kupsch A, Limousin P, Hariz M, Schneider G-H, Yarrow K,  
489            Brown P. 2004 Event-related beta desynchronization in human subthalamic nucleus  
490            correlates with motor performance. *Brain* **127**, 735–746. (doi:10.1093/brain/awh106)
- 491    9.    Fujioka T, Trainor LJ, Large EW, Ross B. 2012 Internalized Timing of Isochronous  
492            Sounds Is Represented in Neuromagnetic Beta Oscillations. *J. Neurosci.* **32**, 1791 LP –  
493            1802. (doi:10.1523/JNEUROSCI.4107-11.2012)
- 494    10.   Kilavik BE, Ponce-Alvarez A, Trachel R, Confais J, Takerkart S, Riehle A. 2012  
495            Context-related frequency modulations of macaque motor cortical LFP beta  
496            oscillations. *Cereb. Cortex* **22**, 2148–2159. (doi:10.1093/cercor/bhr299)
- 497    11.   Khanna P, Carmena JM. 2017 Beta band oscillations in motor cortex reflect neural  
498            population signals that delay movement onset. *Elife* **6**, e24573.  
499            (doi:10.7554/eLife.24573)

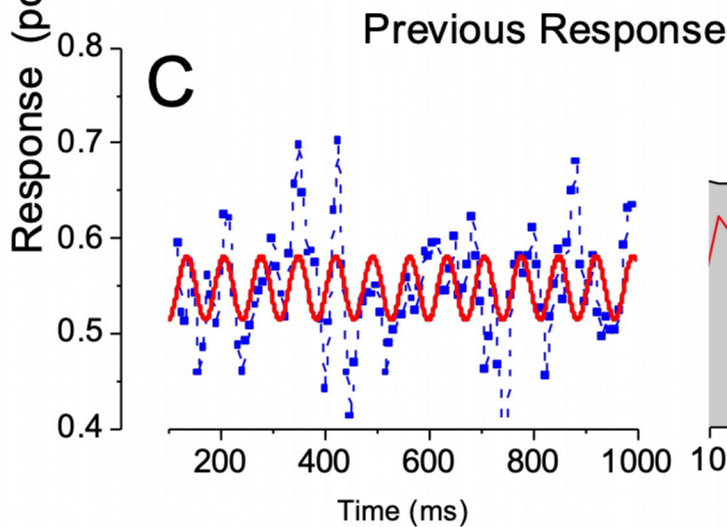
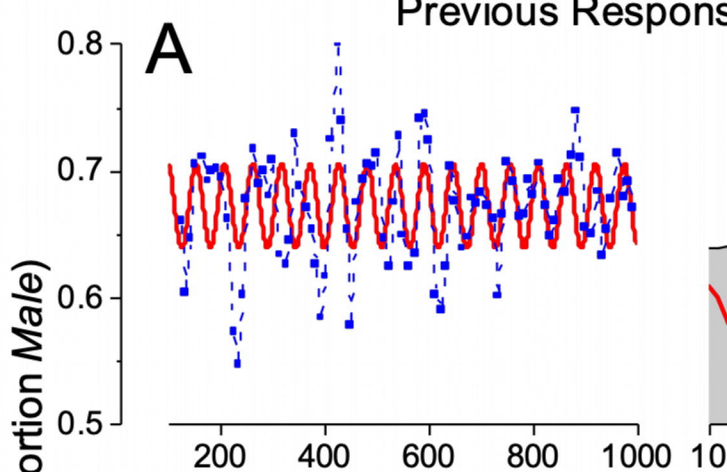
- 500 12. Wagner J, Wessel JR, Ghahremani A, Aron AR. 2018 Establishing a Right Frontal  
501 Beta Signature for Stopping Action in Scalp EEG: Implications for Testing Inhibitory  
502 Control in Other Task Contexts. *J. Cogn. Neurosci.* **30**, 107–118.  
503 (doi:10.1162/jocn\_a\_01183)
- 504 13. Kopell N, Whittington MA, Kramer MA. 2011 Neuronal assembly dynamics in the  
505 beta1 frequency range permits short-term memory. *Proc. Natl. Acad. Sci.* **108**, 3779–  
506 3784. (doi:10.1073/pnas.1019676108)
- 507 14. Hanslmayr S, Staudigl T. 2014 How brain oscillations form memories—A processing  
508 based perspective on oscillatory subsequent memory effects. *Neuroimage* **85**, 648–655.  
509 (doi:10.1016/j.neuroimage.2013.05.121)
- 510 15. Lundqvist M, Rose J, Herman P, Brincat SL, Buschman TJ, Miller EK. 2016 Gamma  
511 and Beta Bursts Underlie Working Memory. *Neuron* **90**, 152–164.  
512 (doi:10.1016/j.neuron.2016.02.028)
- 513 16. Engel AK, Fries P. 2010 Beta-band oscillations--signalling the status quo? *Curr. Opin.*  
514 *Neurobiol.* **20**, 156–165. (doi:10.1016/j.conb.2010.02.015)
- 515 17. Spitzer B, Haegens S. 2017 Beyond the Status Quo: A Role for Beta Oscillations in  
516 Endogenous Content (Re)Activation. *eNeuro* **4**. (doi:10.1523/ENEURO.0170-  
517 17.2017)
- 518 18. Richter CG, Thompson WH, Bosman CA, Fries P. 2017 Top-down beta enhances  
519 bottom-up gamma. *J. Neurosci.* **37**, 6698–6711. (doi:10.1523/JNEUROSCI.3771-  
520 16.2017)
- 521 19. Betti V, Della Penna S, de Pasquale F, Corbetta M. 2021 Spontaneous Beta Band  
522 Rhythms in the Predictive Coding of Natural Stimuli. *Neurosci. a Rev. J. bringing*  
523 *Neurobiol. Neurol. psychiatry* **27**, 184–201. (doi:10.1177/1073858420928988)
- 524 20. Abdalaziz M, Redding Z V, Fiebelkorn IC. 2023 Rhythmic temporal coordination of  
525 neural activity prevents representational conflict during working memory. *Curr. Biol.*  
526 **33**, 1855-1863.e3. (doi:10.1016/j.cub.2023.03.088)
- 527 21. Stokes MG. 2015 ‘Activity-silent’ working memory in prefrontal cortex: a dynamic

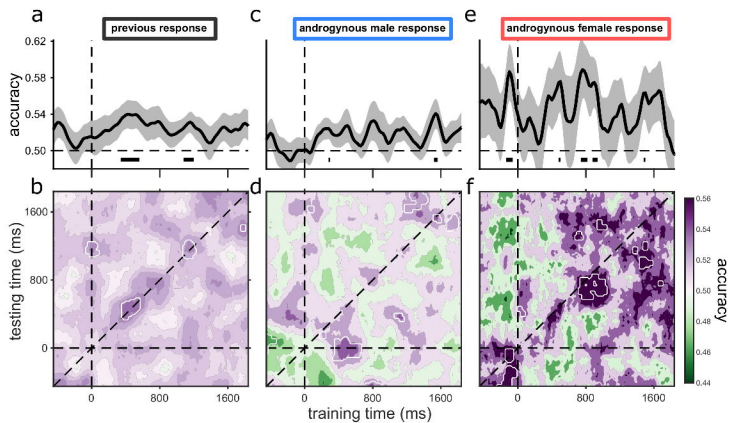
- 528 coding framework. *Trends Cogn. Sci.* **19**, 394–405. (doi:10.1016/j.tics.2015.05.004)
- 529 22. Bae GY, Luck SJ. 2019 Reactivation of Previous Experiences in a Working Memory  
530 Task. *Psychol. Sci.* **30**, 587–595. (doi:10.1177/0956797619830398)
- 531 23. Barbosa J *et al.* 2020 Interplay between persistent activity and activity-silent dynamics  
532 in the prefrontal cortex underlies serial biases in working memory. *Nat. Neurosci.* **23**,  
533 1016–1024. (doi:10.1038/s41593-020-0644-4)
- 534 24. Ranieri G, Benedetto A, Ho HT, Burr DC, Morrone MC. 2022 Evidence of Serial  
535 Dependence from Decoding of Visual Evoked Potentials. *J. Neurosci. Off. J. Soc.*  
536 *Neurosci.* **42**, 8817–8825. (doi:10.1523/JNEUROSCI.1879-21.2022)
- 537 25. Fiser J, Chiu C, Weliky M. 2004 Small modulation of ongoing cortical dynamics by  
538 sensory input during natural vision. *Nature* **431**, 573–578. (doi:10.1038/nature02907)
- 539 26. Myers NE, Rohenkohl G, Wyart V, Woolrich MW, Nobre AC, Stokes MG. 2015  
540 Testing sensory evidence against mnemonic templates. *Elife* **4**, e09000.  
541 (doi:10.7554/eLife.09000)
- 542 27. Sheehan TC, Serences JT. 2022 Attractive serial dependence overcomes repulsive  
543 neuronal adaptation. *PLoS Biol.* **20**, e3001711. (doi:10.1371/journal.pbio.3001711)
- 544 28. Fischer J, Whitney D. 2014 Serial dependence in visual perception. *Nat. Neurosci.* **17**,  
545 738–743. (doi:10.1038/nn.3689)
- 546 29. Kiyonaga A, Scimeca JM, Bliss DP, Whitney D. 2017 Serial Dependence across  
547 Perception, Attention, and Memory. *Trends Cogn. Sci.* **21**, 493–497.  
548 (doi:10.1016/j.tics.2017.04.011)
- 549 30. Cicchini GM, Mikellidou K, Burr DC. 2018 The functional role of serial dependence.  
550 *Proc. R. Soc. B Biol. Sci.* **285**, 20181722. (doi:10.1098/rspb.2018.1722)
- 551 31. Pascucci D, Tanrikulu ÖD, Ozkirli A, Houborg C, Ceylan G, Zerr P, Rafiei M,  
552 Kristjánsson Á. 2023 Serial dependence in visual perception: A review. *J. Vis.* **23**, 9.  
553 (doi:10.1167/jov.23.1.9)
- 554 32. Liberman A, Fischer J, Whitney D. 2014 Serial dependence in the perception of faces.

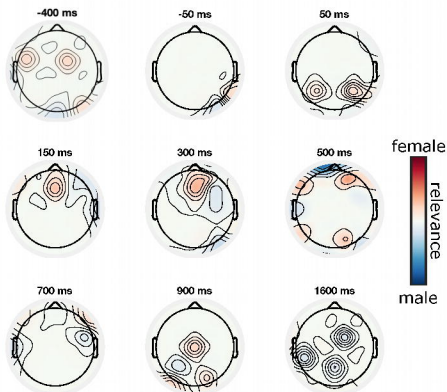
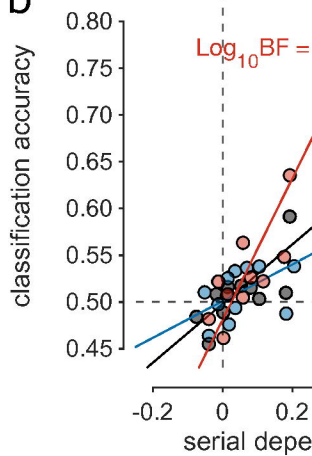
- 555 *Curr. Biol.* **24**, 2569–2574. (doi:10.1016/j.cub.2014.09.025)
- 556 33. Taubert J, Alais D, Burr D. 2016 Different coding strategies for the perception of  
557 stable and changeable facial attributes. *Sci. Rep.* **6**, 32239. (doi:10.1038/srep32239)
- 558 34. Bell J, Burr DC, Crookes K, Morrone MC. 2020 Perceptual Oscillations in Gender  
559 Classification of Faces, Contingent on Stimulus History. *iScience* **23**.  
560 (doi:10.1016/j.isci.2020.101573)
- 561 35. Turbett K, Palermo R, Bell J, Hanran-smith DA, Jeffery L. 2021 Serial dependence of  
562 facial identity reflects high-level face coding. *Vision Res.* **182**, 9–19.  
563 (doi:10.1016/j.visres.2021.01.004)
- 564 36. Zhang H, Morrone MC, Alais D. 2019 Behavioural oscillations in visual orientation  
565 discrimination reveal distinct modulation rates for both sensitivity and response bias.  
566 *Sci. Rep.* **9**, 1–11. (doi:10.1038/s41598-018-37918-4)
- 567 37. Romei V, Gross J, Thut G. 2012 Sounds reset rhythms of visual cortex and  
568 corresponding human visual perception. *Curr. Biol.* **22**, 807–813.  
569 (doi:10.1016/j.cub.2012.03.025)
- 570 38. King J-R, Dehaene S. 2014 Characterizing the dynamics of mental representations: the  
571 temporal generalization method. *Trends Cogn. Sci.* **18**, 203–210.  
572 (doi:10.1016/j.tics.2014.01.002)
- 573 39. Bliss DP, Sun JJ, D’Esposito M. 2017 Serial dependence is absent at the time of  
574 perception but increases in visual working memory. *Sci. Rep.* **7**, 14739.  
575 (doi:10.1038/s41598-017-15199-7)
- 576 40. Ceylan G, Herzog MH, Pascucci D. 2021 Serial dependence does not originate from  
577 low-level visual processing. *Cognition* **212**, 104709.  
578 (doi:10.1016/j.cognition.2021.104709)
- 579 41. Cicchini GM, Benedetto A, Burr DC. 2021 Perceptual history propagates down to  
580 early levels of sensory analysis. *Curr. Biol.* **31**, 1245-1250.e2.  
581 (doi:10.1016/j.cub.2020.12.004)
- 582 42. Fornaciai M, Togoli I, Buetti D. 2023 Perceptual History Biases Are Predicted by Early

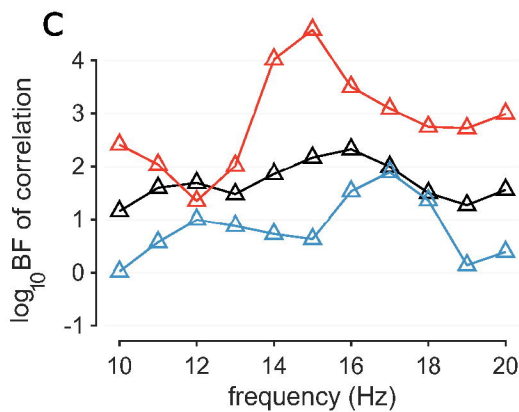
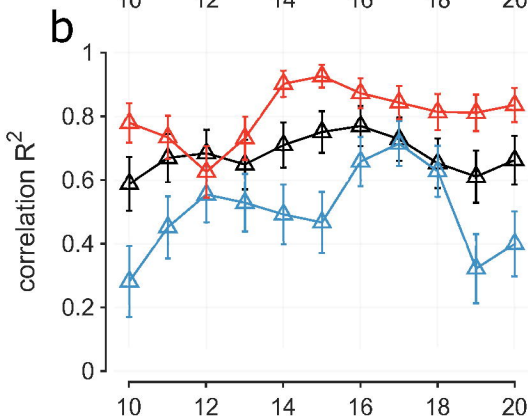
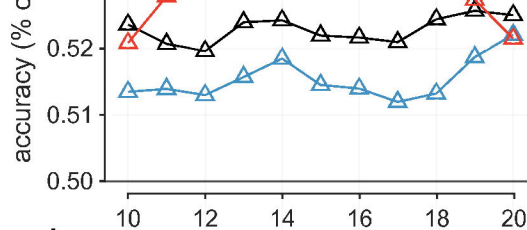
- 583 Visual-Evoked Activity. *J. Neurosci. Off. J. Soc. Neurosci.* **43**, 3860–3875.  
584 (doi:10.1523/JNEUROSCI.1451-22.2023)
- 585 43. Hajonides JE, van Ede F, Stokes MG, Nobre AC, Myers NE. 2023 Multiple and  
586 Dissociable Effects of Sensory History on Working-Memory Performance. *J.*  
587 *Neurosci. Off. J. Soc. Neurosci.* **43**, 2730–2740. (doi:10.1523/JNEUROSCI.1200-  
588 22.2023)
- 589 44. St. John-Saaltink E, Kok P, Lau HC, De Lange FP. 2016 Serial dependence in  
590 perceptual decisions is reflected in activity patterns in primary visual cortex. *J.*  
591 *Neurosci.* **36**, 6186–6192. (doi:10.1523/JNEUROSCI.4390-15.2016)
- 592 45. Cicchini GM, Mikellidou K, Burr D. 2017 Serial dependencies act directly on  
593 perception. *J. Vis.* **17**, 6–6. (doi:10.1167/17.14.6)
- 594 46. Manassi M, Liberman A, Kosovicheva A, Zhang K, Whitney D. 2018 Serial  
595 dependence in position occurs at the time of perception. *Psychon. Bull. Rev.* **25**, 2245–  
596 2253. (doi:10.3758/s13423-018-1454-5)
- 597 47. Masse NY, Yang GR, Song HF, Wang X-J, Freedman DJ. 2019 Circuit mechanisms  
598 for the maintenance and manipulation of information in working memory. *Nat.*  
599 *Neurosci.* **22**, 1159–1167. (doi:10.1038/s41593-019-0414-3)
- 600 48. Runyan CA, Piasini E, Panzeri S, Harvey CD. 2017 Distinct timescales of population  
601 coding across cortex. *Nature* **548**, 92–96. (doi:10.1038/nature23020)
- 602 49. Stokes MG, Kusunoki M, Sigala N, Nili H, Gaffan D, Duncan J. 2013 Dynamic coding  
603 for cognitive control in prefrontal cortex. *Neuron* **78**, 364–375.  
604 (doi:10.1016/j.neuron.2013.01.039)
- 605 50. VanRullen R, Macdonald JSP. 2012 Perceptual echoes at 10 Hz in the human brain.  
606 *Curr. Biol.* **22**, 995–999. (doi:10.1016/j.cub.2012.03.050)
- 607 51. Hao Tam Ho A, Leung J, Burr DC, Alais D. 2017 Auditory Sensitivity and Decision  
608 Criteria Oscillate at Different Frequencies Separately for the Two Ears. *Curr. Biol.* **27**.  
609 (doi:10.1016/j.cub.2017.10.017)
- 610 52. Benedetto A, Morrone MC. 2019 Visual sensitivity and bias oscillate phase-locked to

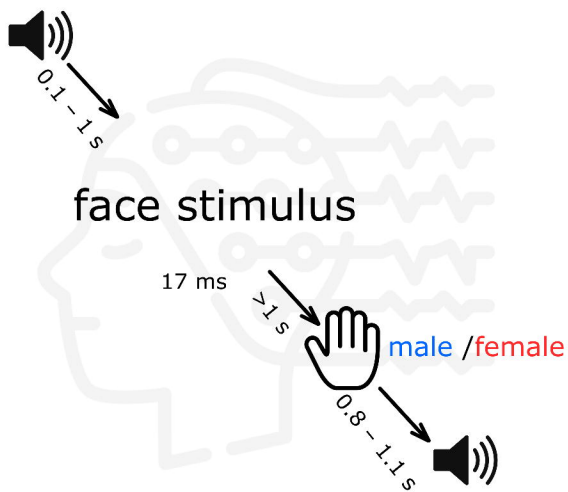
- 611 saccadic eye movements. (doi:10.1167/19.14.15)
- 612 53. Benedetto A, Charles Burr D, Morrone MC, Stella-Maris I, Tirreno V Del,  
613 Calambrone I. 2018 Sensory and Motor Systems Perceptual Oscillation of Audiovisual  
614 Time Simultaneity. (doi:10.1523/ENEURO.0047-18.2018)
- 615 54. Romei V, Driver J, Schyns PG, Thut G. 2011 Rhythmic TMS over parietal cortex links  
616 distinct brain frequencies to global versus local visual processing. *Curr. Biol.* **21**, 334–  
617 337. (doi:10.1016/j.cub.2011.01.035)
- 618 55. Liu L, Luo H. 2019 Behavioral oscillation in global/local processing: Global alpha  
619 oscillations mediate global precedence effect. *J. Vis.* **19**, 12. (doi:10.1167/19.5.12)
- 620 56. Cabral J, Castaldo F, Vohryzek J, Litvak V, Bick C, Lambiotte R, Friston K,  
621 Kringelbach ML, Deco G. 2022 Metastable oscillatory modes emerge from  
622 synchronization in the brain spacetime connectome. *Commun. Phys.* **5**, 184.  
623 (doi:10.1038/s42005-022-00950-y)
- 624 57. Bastos AM, Loonis R, Kornblith S, Lundqvist M, Miller EK. 2018 Laminar recordings  
625 in frontal cortex suggest distinct layers for maintenance and control of working  
626 memory. *Proc. Natl. Acad. Sci.* **115**, 1117–1122. (doi:10.1073/pnas.1710323115)
- 627 58. Jung T-P, Humphries C, Lee TW, McKeown MJ, Iragui V, Makeig, Sejnowski TJ.  
628 2000 Removing electroencephalographic artifacts from by blind source separation.  
629 *Psychophysiology* **37**, 163–178.
- 630





**a****b**



**a****b**